Multichannel filters via Γ-*M* and Γ-*K* waveguide coupling in two-dimensional triangular-lattice photonic crystal slabs

Ya-Zhao Liu,[1,a)] Rong-Juan Liu,[1] Shuai Feng,[1] Cheng Ren,[1] Hai-Fang Yang,[2] Dao-Zhong Zhang,[1] and Zhi-Yuan Li[1,b)]
[1]*Laboratory of Optical Physics, Beijing National Laboratory for Condensed Matter Physics, Institute of Physics, Chinese Academy of Sciences, Beijing 100190, China*
[2]*Laboratory of Micro Fabrication, Institute of Physics, Chinese Academy of Sciences, Beijing 100190, China*

(Received 4 September 2008; accepted 22 November 2008; published online 16 December 2008)

We demonstrate the design, fabrication, and characterization of a multichannel filter in a two-dimensional triangular-lattice photonic crystal slab. The output signal channel, which directs in the Γ-*M* crystalline direction, is orthogonal to the input signal channel that directs in the Γ-*K* crystalline direction. In each channel, the filtering function is guaranteed by the indirect resonant coupling between the waveguide and the cavity. Four resonant cavities with different sizes provide the mechanism of finely tuning the output wavelength. Our experimental results are in good agreement with simulations. © *2008 American Institute of Physics*. [DOI: 10.1063/1.3052687]

Two-dimensional (2D) photonic crystal (PC) slab structures with triangular lattice were extensively studied.[1–3] Linear and point defects are introduced in the PC platform to form waveguides and cavities, from which various integrated optical elements and devices can be built.[4–6] Channel drop filters work on resonant coupling between cavities and input/output waveguides either in pure 2D PCs[7,8] or in more practical 2D PC slabs.[9–15] The side-coupled technique was extensively studied to construct in-plane channel drop filters in the 2D PC slab platform.[10–15] Based on the modal theories, heterogeneous structures were used to enhance coupling efficiency in high-performance channel-drop filters.[11–13]

In almost all of the previous works, the PC waveguide channels were always placed in the Γ-*K* direction of the triangular-lattice photonic crystal and waveguides along other crystalline directions have been largely neglected. The angle between two neighboring Γ-*K* directions leads to a 60° or 120° bend in coupling. Although Γ-*K* waveguides in different equivalent crystalline directions suffice to form an integrated optical circuit composed of interconnected waveguide network and various types of channel drop filters in the entire 2D plane of photonic crystals, it is desirable to consider other geometries of interconnecting and coupling for the sake of more freedoms and flexibilities in implementing integrated functionality. In this paper, we propose a type of PC filter based on the combination of two orthogonal crystalline directions, the Γ-*M* and Γ-*K* directions, in a triangular lattice photonic crystal. The two directions are used as the input and output signal channels respectively, and they are connected via cavity resonance.

The two waveguide directions in a triangular lattice crystal are illustrated in Fig. 1(a) and labeled with Γ-*K* and Γ-*M*. The angle between the Γ-*K* direction and the Γ-*M* direction is 90°. Since the period in the Γ-*M* direction turns out to be $a'=\sqrt{3}a$ (a is the lattice constant of the crystal), and there is no natural pathway existing along this direction, the waveguides cannot be formed by just removing a line of lattice points. However, four adjacent lattice points along this direction form a diamond area. By removing a line of diamond areas, we can obtain a clusterlike waveguide (similar to a coupled-cavity waveguide). The scanning electron microscopy (SEM) pictures of such Γ-*M* waveguide before and after optimization for good transmission properties are displayed in Figs. 1(b) and 1(c), respectively.

A three-dimensional finite-difference time-domain (FDTD) method was employed to calculate the modal dispersion relation of the original Γ-*M* waveguide modes. The dispersion curves of the transverse-electric (TE)-like modes are plotted in Fig. 2(a). Here the refractive index of the material is 3.4, the lattice constant is $a=430$ nm, the radii of the air holes is $r_0=120$ nm, and the thickness of the slab is $h=220$ nm. The band gap of the crystal in the Γ-*M* direction ranges from 0.45 to 0.54 c/a', where c is the velocity of light in vacuum. The propagating waveguide modes are within the dashed box, and the band width is 22 nm. This value is consistent with the transmission spectrum simulation. We have found that this narrow band can be greatly broadened by modifying the radii of the air holes along the pathway, as has been depicted in Fig. 1(a). A transmission window of nearly 74 nm as shown in Fig. 2(b) is obtained by shrinking the size of the innermost air holes ($r_1=50$ nm) and enlarging the size of those next to them ($r_2=170$ nm).

Next we construct cavities to efficiently connect the input Γ-*K* and output Γ-*M* channels. We find that the geometry

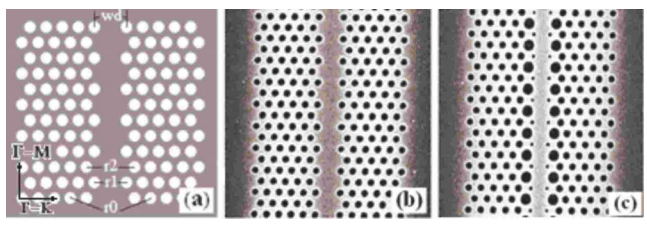

FIG. 1. (Color online) (a) Schematic of Γ-*M* waveguide constructed in a triangular-lattice PC slab. The width of the waveguide w_d, as well as the radius of air holes in the first and second row (r_1 and r_2), are the three crucial parameters to optimize the width of the transmission windows. (b) and (c) are SEM pictures of original and optimized Γ-*M* waveguides.

a)Electronic mail: liuyazhao@aphy.iphy.ac.cn.
b)Electronic mail: lizy@aphy.iphy.ac.cn.

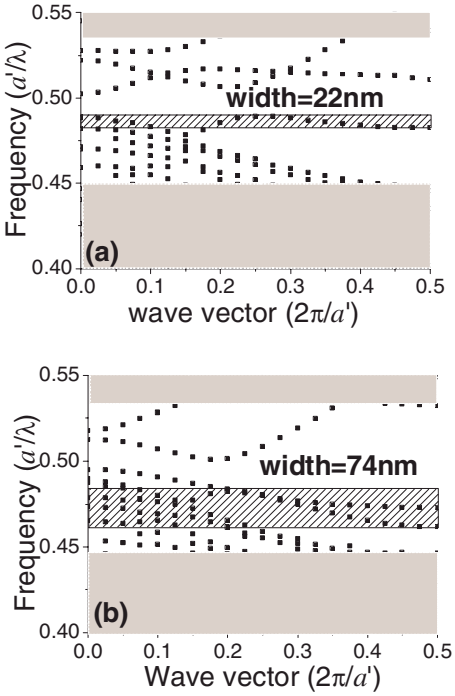

FIG. 2. (Color online) Calculated modal dispersion relation of (a) the original Γ-*M* waveguide and (b) an optimized Γ-*M* waveguide. The band width of the waveguide modes (within the dashed boxes) is 22 nm in the original waveguide. After optimization it is significantly broadened to 74 nm.

of missing holes leads to an effective coupling cavity based on the large enough space to support resonance and the defect along the Γ-*M* direction is a better choice than the Γ-*K* direction because its wave vector coincides with the output direction. Three holes located in the Γ-*M* direction are removed to form an effective resonant cavity, as schematically shown in Fig. 3(a). The transmission spectrum of such structure was simulated by the 2D FDTD method with an effective index approximation, and the result is shown in Fig. 3(b). Only one resonant peak occurs at the wavelength of 1568 nm. An experimental device fabricated by focused ion beam lithographic technique has been tested. Figure 3(c) illustrates the experiment images of the infrared signal for the device that were recorded by an optical microscopy. From the bright spot of light transferred from the in-plane orientation to the vertical orientation due to scattering, it is obvious that the signal has dropped from the input Γ-*K* channel into the output Γ-*M* channel when it is at on-resonance wavelength and disappears when it is at off-resonance. In the on-resonance case, a bright spot is still observed at the transmission port in addition to at the drop port. This is attributed to the incomplete drop of signal from the input channel to the drop channel via cavity resonance. To facilitate better coupling efficiency, heterostructures in the input waveguide channel can be adopted to cause recycling of energy power dropping from each segment of the input waveguide into the corresponding output channel via cavity resonance as in Refs. 11–13.

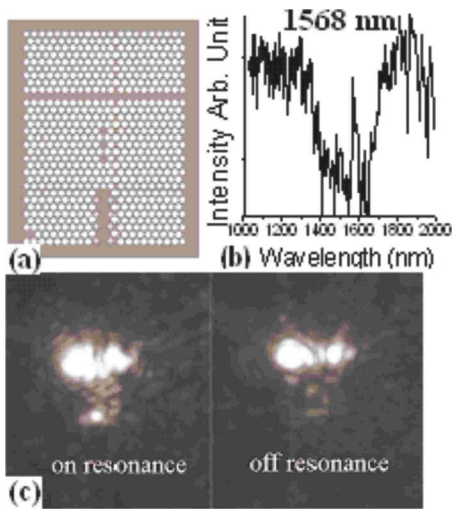

FIG. 3. (Color online) (a) Schematic configuration of an optical filter consisting of the Γ-*K* and Γ-*M* waveguides serving as the input and output channels, and the microcavity made from three missing air holes serving as the resonant coupler. (b) Calculated transmission spectrum at the output channel in the linear scale. (c) Infrared imaging of the output signal observed in experiment for a practical sample. A bright spot appears at the end of the output channel when the input wavelength coincides with the resonant wavelength and disappears when it is at off-resonance.

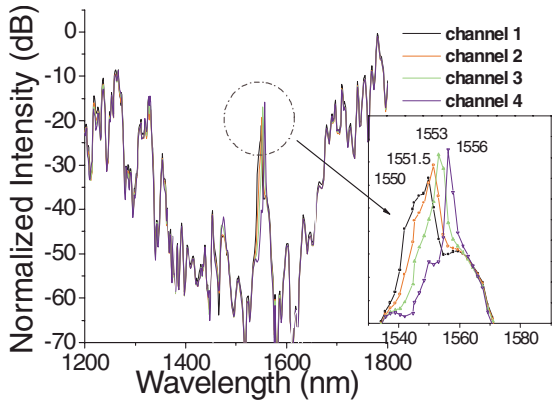

FIG. 4. (Color online) Transmission spectra of the four-channel filter simulated by the 2D FDTD method. The amplified picture of spectrum in the inset indicates the details at the resonance. Each channel has only one resonant peak, which appears at 1550, 1551.5, 1553, and 1556 nm, respectively.

We construct a four-channel filter by adopting four cavities whose size is finely changed by moving the end points of the cavity (marked with "a,b" and "c,d" as shown in the inset of Fig. 5) outward from 0 to 15 nm with a step of 5 nm. Other parameters are of $r_1=90$ nm and $r_2=190$ nm. The Γ-*M* waveguide supports a large enough transmission band with width of 40 nm. Figure 4 shows the simulated spectrum of each channel by means of the 2D FDTD technique. In the

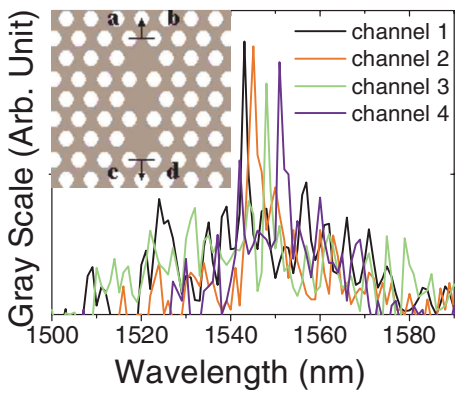

FIG. 5. (Color online) SEM image of the fabricated four-channel filter. Four cavities are located on the two sides of the input Γ-*K* waveguide. The parameters of the Γ-*M* waveguide are $r_1=90$ nm and $r_2=190$ nm.

TABLE I. Structural parameters of the four-channel filter.

	End points moving distance (nm)	Theoretical resonant peak (nm)	Measured resonant peak (nm)	Theoretical distance from channel 1 (nm)	Experimental distance from channel 1 (nm)	Relative distance deviation (nm)
Channel 1	0	1550	1543			
Channel 2	5	1551.5	1545	1.5	2	0.5
Channel 3	10	1553	1548	3	5	2
Channel 4	15	1556	1551	6	8	2

entire gap region there is only one resonant wavelength for each of the four channels. A closer examination over the spectrum data indicates that the approximate interval of adjacent peaks is about 1.5 nm, and the resonant peaks shift to lower frequency as the displacement of the end points increases.

The designed orthogonal-coupling four-channel filter was realized experimentally in a silicon air-bridged slab by means of electron-beam lithography and inductively coupling plasma etching techniques. The input and output end of the major signal channel (Γ-K waveguide) are connected to tapered ridge waveguides. The output channels were cut with shallow grooves to enhance the light scattering at the output channel. The SEM picture in Fig. 5 illustrates the geometry of the device in detail. A tunable laser ranging from 1500 to 1640 nm serves as the light source. The incident light was injected from free space into one facet of the ridge waveguide via a lensed fiber then transmitted through the photonic crystal structure and emitted from the output channel. The transmission intensity is normalized by comparing with a ridge waveguide with same length and width. We used an optical charge-coupled device microscopy to illustrate the experiment images of the infrared signal and transform them into gray scale to get the relative intensity, which is very important for us to investigate the characterization of this filter. Table I outlines the parameters of the device. In our experiment, four resonant peaks were found to appear at the wavelength of 1543, 1545, 1548, and 1551 nm, as shown in Fig. 6. Theoretical simulations and experimental results are listed in Table I for comparison. In spite of slight shift in the resonant peak toward higher frequency, which we believe is induced by the uncertainties in the fabrication, the experimental results are in fairly good agreement with the simulation results, where the maximum relative deviation of resonant wavelength is within 2 nm.

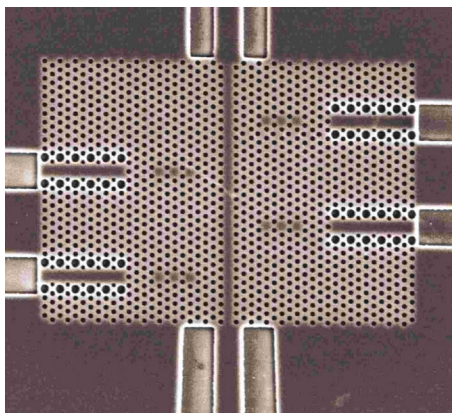

FIG. 6. (Color online) Experimental transmission spectra of the four-channel filter in linear scale. The inset picture illustrates two groups of end points (air-hole centers) of the cavity marked with "a, b" and "c, d." Black arrows indicate the moving direction of these air holes.

In summary, we have demonstrated a multichannel filter in 2D triangular-lattice PC slab that is made from a usual input Γ-K waveguide channel orthogonally coupled through microcavities with the output waveguide channels that are along the Γ-M direction. The Γ-M waveguide is delicately designed to have a wide-band transmission property. Based on the design, we have fabricated a four-channel filter on the silicon thin slab where the fine frequency tuning (below 2 nm) can be realized by changing the size of the microcavity. Good agreement between theory and experiment is obtained. These results clearly demonstrate that the designed Γ-M waveguides can act together with the usual Γ-K waveguide to construct high-performance multichannel filers with more structural flexibility.

This work is supported by the National Key Basic Research Special Foundation of China (Grant Nos. 2007CB613205 and 2006CB921702) and the National Natural Science Foundation of China (Grant No. 10525419).

[1] S. G. Johnson, S. Fan, P. R. Villeneuve, J. D. Joannopoulos, and L. A. Kolodziejski, Phys. Rev. B **60**, 5751 (1999).
[2] E. Yablonovitch, Science **289**, 557 (2000).
[3] S. Noda, A. Chutinan, and M. Imada, Nature (London) **407**, 608 (2000).
[4] L. H. Frandsen, P. I. Borel, Y. X. Zhuang, A. Harpoth, M. Thorhauge, and M. Kristensen, Opt. Lett. **29**, 1623 (2004).
[5] A. Talneau, L. LeGouezigou, N. Bouadma, M. Kafesaki, C. M. Soukoulis, and M. Agio, Appl. Phys. Lett. **80**, 547 (2002).
[6] M. Notomi, A. Shinya, S. Mitsugi, E. Kuramochi, and H. Y. Ryu, Opt. Express **12**, 1551 (2004).
[7] S. H. Fan, P. R. Villeneuve, J. D. Joannopoulos, and H. A. Hau, Phys. Rev. Lett. **80**, 960 (1998).
[8] M. Qiu and B. Jaskorzynska, Appl. Phys. Lett. **83**, 1074 (2003).
[9] Y. Akahane, T. Asano, B. S. Song, and S. Noda, Appl. Phys. Lett. **83**, 1512 (2003).
[10] H. Takano, Y. Akahane, T. Asano, and S. Noda, Appl. Phys. Lett. **84**, 2226 (2004).
[11] H. Takano, B.-S. Song, T. Asano, and S. Noda, Opt. Express **14**, 3491 (2006).
[12] A. Shinya, S. Mitsugi, E. Kuramochi, and M. Notomi, Opt. Express **13**, 4202 (2005).
[13] A. Shinya, S. Mitsugi, E. Kuramochi, and M. Notomi, Opt. Express **14**, 12394 (2006).
[14] C. Ren, J. Tian, S. Feng, H. H. Tao, Y. Z. Liu, K. Ren, Z. Y. Li, B. Y. Cheng, and D. Z. Zhang, Opt. Express **14**, 10014 (2006).
[15] Y. Z. Liu, S. Feng, J. Tian, C. Ren, H. H. Tao, Z. Y. Li, B. Y. Cheng, and D. Z. Zhang, J. Appl. Phys. **102**, 043102 (2007).

Γ–M waveguides in two-dimensionaltriangular-lattice photonic crystal slabs

Ya-Zhao Liu, Rong-Juan Liu, Chang-Zhu Zhou, Dao-Zhong Zhang, and Zhi-Yuan Li*

Institute of Physics, Chinese Academy of Sciences, P.O. Box 603, Beijing 100190, China
**Corresponding author: lizy@aphy.iphy.ac.cn*

Abstract: We propose a line defect waveguide structure along the Γ–M direction in two-dimensional triangular lattice silicon photonic crystal slabs. The modal dispersion relation and the transmission spectra of this waveguide are studied. The results show that by perturbing the width of the line defect and the diameter of the air holes adjacent to the waveguide core, one can control the width of the single mode transmission window and make it far broader than the original one. The proposed Γ–M waveguide will help to build a more flexible network of interconnection channel of light in two-dimensional photonic crystal slabs.

OCIS codes: (230.5298) Photonic crystals; (130.5296) Photonic crystal waveguides; (130.2790) Guided waves; (230.3990) Microstructure devices;

References and links

1. E. Yablonovitch, "How to be truly photonic," Science **289**, 557-559 (2000).
2. S. G. Johnson, S. Fan, P. R. Villeneuve, J. D. Joannopoulos, and L. A. Kolodziejski, "Guided modes in Photonic crystal slabs," Phys. Rev. B **60**, 5751-5758 (1999).
3. S. Noda, A. Chutinan, and M. Imada, "Trapping and emission of photons by a single defect in a photonic bandgap structure," Nature **407**, 608-610 (2000).
4. H. Takano, B. S. Song, T. Asano, and S. Noda, "Highly efficient in-plane channel drop filter in a two-dimensional heterophotonic crystal," Appl. Phys. Lett. **86**, 241101 (2005).
5. A. Shinya, S. Mitsugi, E. Kuramochi, and M. Notomi, "Ultrasmall multi-channel resonant-tunneling filter using mode gap of width-tuned photonic-crystal waveguide," Opt. Express **13**, 4202-4208 (2005).
6. B. S. Song, T. Asano, Y. Akahane, Y. Tanaka and S. Noda, "Multichannel add/drop filter based on in-plane hetero photonic crystals," IEEE J. Lightwave Technol. **23**, 1449-1455 (2005).
7. H. Takano, B. S. Song, T. Asano, S. Noda, "Highly efficient multi-channel drop filter in a two-dimensional hetero photonic crystal**,"** Opt. Express **14**, 3491-3496 (2006).
8. C. Ren, J. Tian, S. Feng, H. H. Tao, Y. Z. Liu, K. Ren, Z. Y. Li, B. Y. Cheng, and D. Z. Zhang, "High resolution three-port filter in two dimensional photonic crystal slabs," Opt. Express **14**, 10014-10020 (2006).
9. Y. Akahane, T. Asano, B. S. Song and S. Noda, "Fine-tuned high-*Q* photonic-crystal nanocavity," Opt. Express **13**, 1202-1214 (2005).
10. B. S. Song, S. Noda, T. Asano and Y. Akahane, "Ultra-high-Q photonic double-heterostructure nanocavity," Nature Mater. **4**, 207-210 (2005).
11. T. Asano, B. S. Song, and S. Noda, "Analysis of the experimental Q factors (~ 1 million) of photonic crystal nanocavities," Opt. Express **14**, 1996-2002 (2006).
12. M. Notomi, K. Yamada, A. Shinya, J. Takahashi, C. Takahashi, and Yokohama, "Extremely large group-velocity dispersion of line-defect waveguides in photonic crystal slabs," Phys. Rev. Lett. **87**, 253902 (2001).
13. M. Notomi, A. Shinya, K.Yamada, J. Takahashi, C. Takahashi and I. Yokohama, "Singlemode transmission within photonic bandgap of width-varied single-line-defect photonic crystal waveguides on SOI substrates," Electron. Lett. **37**, 293-295 (2001).
14. K. Yamada, H. Morita, A. Shinya and M. Notomi, "Improved line-defect structures for photonic crystal waveguides with high group velocity," Opt. Commun. **198**, 395-402 (2001).

#101332 - $15.00 USD Received 9 Sep 2008; revised 10 Oct 2008; accepted 25 Nov 2008; published 15 Dec 2008

15. M. Notomi, A. Shinya, K. Yamada, J. I. Takahashi, C. Takahashi, and I. Yokohama, "Structural tuning of guiding modes of line-defect waveguides of silicon-on-insulator photonic crystal slabs," IEEE J. Quantum Electron **38**, 736-742 (2002).
16. L. H. Frandsen, A. V. Lavrinenko, J. Fage-Pedersen, and I. Borel, " Photonic crystal waveguides with semi-slow light and tailored dispersion properties," Opt. Express **14**, 9444-9450 (2006).
17. B.-S. Song, T. Asano and S. Noda, "Heterostructures in two-dimensional photonic-crystal slabs and their application to nanocavities," J. Phys. D **40**, 2629-2634 (2007).
18. Y. Z. Liu, S. Feng, J. Tian, C. Ren, H. H. Tao, Z. Y. Li, B.Y. Cheng, and D. Z. Zhang, "Mulitchannel filters with shape designing in two-dimensional photonic crystal slabs," J. Appl. Phys. **102**, 043102 (2007).
19. J. D. Joannopoulos, R. D. Meade, and J. N. Winn, *Photonic Crystals* (Princeton University Press, Princeton, (1995).
20. D. Gerace and L. C. Andreani, "Low-loss guided modes in photonic crystal waveguides," Opt. Express **13**, 4939 (2005).

1. Introduction

Photonic crystals (PCs) have attracted great attention for many years due to their strong power in controlling the motion of photons. The periodical structures in these materials enable the creation of photonic band gaps (PBGs) to insulate light transmission [1-3]. Among various kinds of PCs, two-dimensional (2D) PC slabs have been studied most extensively as a possible candidate for future photonic integrated circuits due to relative ease for current micro-fabrication technologies to build these structures in the near infrared wavelengths. 2D triangular-lattice PC slab structures are known to possess a large PBG for the TE-like polarization mode and it is technologically convenient to incorporate various defects into them [4-8]. Usually, point defects work as micro-cavities with high-Q factor [9-11] and line defects serve as waveguide channels for light to propagate efficiently and freely. In previous works, single-mode or multi-mode optical waveguides are usually made by removing one or more rows of air holes along the Γ–K direction in the triangular lattice PC. It has been proved in plenty of works that the number of waveguide modes as well as the width of the transmission windows (which is equal to the total band width of all guided modes together) can be controlled by tuning the core width of the line defects [12-18]. However, waveguides along other directions in the triangular lattice PC, at least to our knowledge, were rarely discussed. Just like the Γ–K direction, waveguides along the Γ–M direction should also be able to guide confined mode due to the existence of a complete 2D PBG in the 2D triangular lattice PC. A large degree of freedom can be further explored to incorporate line defects in this crystalline direction. In this paper, we report a method for making line defects along the Γ–M direction and analyze the optical properties of such waveguides. Simulations and experiments show that the waveguide modes in these line defects can be properly tuned by changing the geometrical parameters such as the width of the waveguide core and radius of the air holes around the core. Our work for the first time shows that high-performance Γ–M waveguides can be successfully realized in the 2D triangular lattice PC slab.

2. Original Γ–M waveguides

The two directions in the triangular lattice for creating waveguides are illustrated in Fig. 1 and labeled with Γ–K and Γ–M. The waveguides along the Γ–K direction can be naturally formed by removing one or several lines of lattice points along this direction [19], but this method does not work well for the Γ–M direction because there is no natural pathway along this direction. Fortunately, after careful observation we find that the four neighboring lattice points along this direction compose a diamond region, as illustrated in Fig. 1(a). By removing a line of diamond areas, we can obtain a cluster-like waveguide along the Γ–M direction as depicted in Fig. 1(b). This waveguide is called the original Γ–M waveguide.

#101332 - $15.00 USD Received 9 Sep 2008; revised 10 Oct 2008; accepted 25 Nov 2008; published 15 Dec 2008

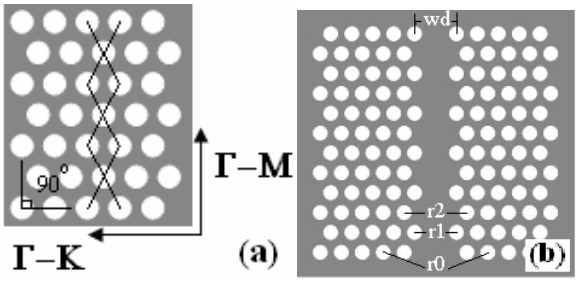

Fig. 1. Schematic image of a triangular lattice photonic crystal slab with waveguides. The original Γ–M waveguide as illustrated in panel (b) is formed by removing a line of diamond pattern of lattice points as depicted in panel (a) along the Γ–M crystalline direction.

Before going on with our analysis of this line defect, it is important to first have a clear knowledge of the PBG property of the background PC structure. We choose the typical parameters for silicon 2D PC slab working at near infrared wavelengths: the lattice constant is a=430 nm, the radius of air holes is r_0=120 nm (0.28a) and the thickness of the slab is 220 nm (0.51a). We have employed the three-dimensional (3D) finite-difference time-domain (FDTD) method to solve the band diagram for both the background crystal and the waveguide. Since the period of the crystal in the Γ–M direction is $a' = \sqrt{3}a$, we use normalized frequency (a'/λ) and wave vector k in unit of ($2\pi/a'$) to describe the band diagram. The calculated modal dispersion relation and modal field profile of guided modes in the original Γ–M waveguide are displayed in Fig. 2(a) and Fig. 3(a). The figure indicates that a 2D PBG opens in the 0.45-0.54 (a'/λ) frequency window. The solid red line represents the edge of the light cone for the 2D PC slab. Since the period of the Γ–M waveguide turns out to be $\sqrt{3}$ times of the lattice constant, the slope of the light line is much more close to the Brillouin zone edge of the k vector than the conventional Γ–K waveguide. Figure 2(a) shows that the original Γ–M waveguide has two guided modes within the PBG, which are defined as even and odd modes based on the symmetry of their E_y field component with respect to the mirror reflection plane passing through the waveguide central axis. Since the light line is so close to the Brillouin zone edge, the bands of the guided modes become flat and limited under the light cone, which theoretically leads to very narrow transmission window of several nanometers (below 5 nm) and make the waveguide susceptible to structural disorders.

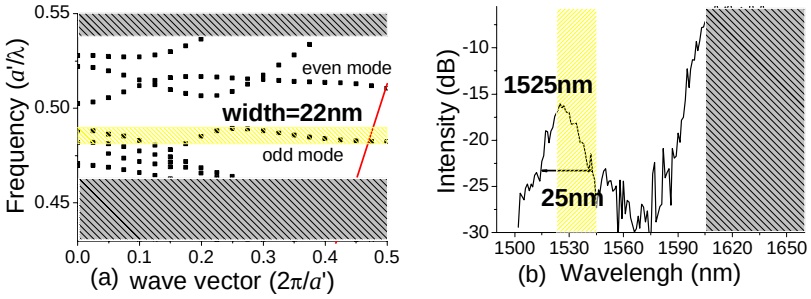

Fig. 2. (a). Calculated dispersion relation and (b) measured transmission spectra of guided modes in the original Γ-M waveguides (with parameters of a=430nm, r_1 = r_2=120nm, and w_0=2a). The width of the transmission window is 22nm. The red line in panel (a) represents the light line, and the yellow shadow region in panel (b) represents the theoretical mode band.

In order to make clear of this issue, we investigate the performance of waveguides by experiment. The designed waveguide pattern was drawn on the top layer of silicon-on-

#101332 - $15.00 USD Received 9 Sep 2008; revised 10 Oct 2008; accepted 25 Nov 2008; published 15 Dec 2008

insulator (SOI) wafer by electron-beam lithography, and then transferred to the silicon slab by inductively-coupled-plasma dry-etching. The insulator layer (SiO_2) underneath the silicon pattern region was removed by wet-etching to form an air-bridged structure, which facilitates the tightest vertical confinement for photons. Each sample had a tapered silicon ridge waveguide as an input port to improve the coupling efficiency of the signal from the fiber into the PC waveguide. The length of the PC waveguide sample was deliberately set to be 20 μm in order to show the effect of the "leaky" modes and avoid the problem of mechanic fragility caused by air-bridge structure. The scanning electron microscope (SEM) image of the fabricated sample is shown in the upper panel of Fig. 4. The input optical signal came from a continuous wave tunable semiconductor laser with the wavelength ranging from 1500 to 1640 nm, launched into one facet of the ridge waveguide via a single-mode lensed fiber. Power meter was used to detect the optical signals transmitted through the waveguide and emitted from the output side. The measurement was made with TE polarization and normalized by a ridge waveguide on silicon with same length and width. Figure 2(b) shows the measured transmission spectrum of the Γ–M waveguides. There is only one transmission band in the whole tested region, which is highlighted by the yellow gray shadow area. We also use the gray yellow area to denote the corresponding pass band in the theoretical band diagram in Fig. 2(a). The simulated center and the width of the mode region are 1533nm and 22nm, while these parameters are 1524nm and 25nm for the practical sample. Despite a frequency deviation caused by the uncertainties in the fabrication process, the observed high transmission band coincides well with theory. Notice that this high transmission band consists of a large fraction of "leaky" modes that lie above the light line of the waveguide in addition to those guided modes that lie below the light line which should be truly lossless in principle. In other words, the leaky modes have a larger bandwidth than the lossless guided modes. It seems that the "leaky" mode above the light cone doesn't "leak" for the 20 um long Γ–M waveguide, or at least, these "leaky" modes are low loss modes and still can propagate for a long path.

3. Optimized Γ–M waveguides

With the contribution of the seemingly "leaky" but actually low loss mode, the width of the transmission window is greatly broadened compared with the very limited guided mode band lying below the light line. However it is still not broad enough to accomplish practical applications. The narrow band features of the original Γ–M waveguide can be understood when we take a closer look at the geometric configuration of the waveguide. The waveguide has very rough walls and in some sense it can be assumed to be a coupled cavity waveguide made from a series of cavity-like diamond regions in Fig. 1(a). The distance between adjacent cavities is a'. The transportation of light through the waveguide is obstructed by the two protruding air holes of each diamond region and this results in the slow group velocity and flat band of the waveguide. In comparison, the usual Γ–K waveguide [made by removing one row of air holes along the Γ–K direction, as can be visualized in Fig. 1(a)] has much smoother walls and the light propagation pathway has little obstruction, leading to a much wider guided-mode band and much larger group velocity of light through the waveguide than the Γ–M waveguide. Similar ideas have been adopted in analyzing and designing optimal Γ–K waveguides with large group velocities and wide transmission windows [14]. The above analysis in fact has suggested an appropriate way to modify the original Γ–M waveguide so that its transportation properties, in particular the guided-mode band width can be improved as much as possible: The walls of the waveguide should be made as smooth as possible. In the following we will show that such an intuition is efficient and effective in designing high-performance Γ–M waveguides.

To realize effective PBG waveguides, it is desirable to have confined waveguide modes

#101332 - $15.00 USD Received 9 Sep 2008; revised 10 Oct 2008; accepted 25 Nov 2008; published 15 Dec 2008

with sufficiently broad transmission windows within the PBG region and a wide-band single mode operation is most preferred. To have a better idea on how a particular structural perturbation on the original Γ–M waveguide will affect the guided mode, we look more closely at the modal field profile of the two guided modes as displayed in Fig. 3(a). The corresponding k vector for these two modes are both 0.4 ($2\pi/a'$). The modal field of the two eigenmodes penetrates into the photonic crystal cladding and concentrates at the first and second row of air holes, thus it suffices to only consider some perturbations on the geometric parameters of air holes in these two rows in order to optimize the transmission band width of the guided modes.

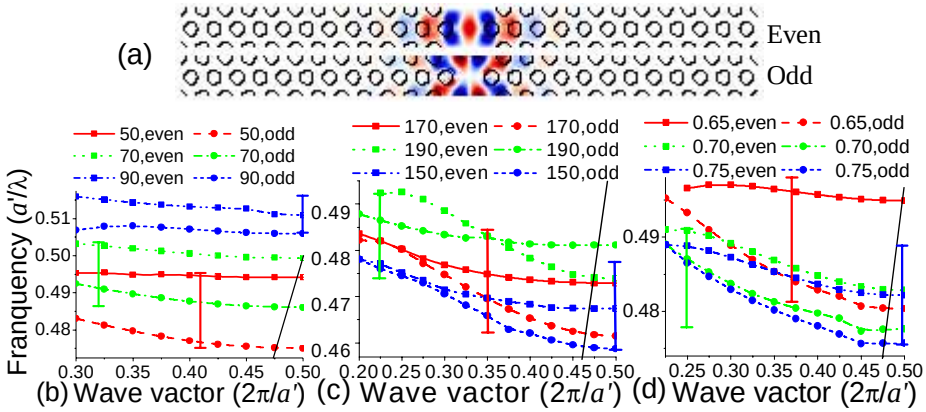

Fig. 3. (a). Calculated modal field profile for the even (upper plot) and odd (lower plot) guided mode and dispersion relation of guided modes in the modified waveguide structures by varying the parameters of (b) r_1, (c) r_2, and (d) w_d. In panel (b), r_2=120nm, w_d =0.75 w_0, r_1 varies from 0 to 90nm. In panel (c), r_1=50nm, w_d =0.75 w_0, r_2 varies from 150 to 190nm. In panel (d), r_1=50nm, r_2=170nm, w_d varies from 0.65 w_0 to 0.75 w_0. The black lines in panels represent the light line.

As illustrated in Fig. 1(b), we define the radius of air holes in the first and second rows as r_1 and r_2. The width of the waveguide w_d is defined by the spacing between the centers of the nearest air holes on the two sides of the waveguides, w_0=2a=860nm represents the width of the original Γ–M waveguide. Since the waveguide can be assumed as a connection of a periodic array of little microcavities, it is necessary to break the cavities and make the channel a smooth pathway. A natural way to achieve this aim is to shrink the size of the air holes in the first row and enlarge the size of the air holes in the second row. At the same time the width of the waveguide w_d can be changed from the value of w_0.

The 3D FDTD method is used again to investigate the underlying principle of optimization by looking at the band diagram of different perturbed Γ–M waveguides. Firstly, we vary r_1 from 50 nm to 90 nm (0.12a to 0.2a) with a step of 20 nm (0.04a). The other structural parameters are fixed as r_2= r_0=120 nm (0.28a) and w_d =0.75 w_0. The calculation result of dispersion curves is basically consistent with our hypothesis. Figure 3(b) clearly shows that the width and position of the entire waveguide mode strongly depend on r_1. The odd mode increases its band width from 6 to 45 nm, but the even mode just exhibits a small increase in width (below 3 nm). The decrease in r_1 has resulted in an apparent increase in the transmission band width. Similar operation is made on the air holes in the second row. We fix r_1=50 nm (the optimal value) and w_d=0.75 w_0 and increase r_2 from 150 nm to 190 nm (0.35a to 0.44a) with a step of 20 nm. As can be found from Fig. 3(c), the width of the transmission window reaches the maximum quantity at r_2=170 nm (0.4a). On the contrary to

#101332 - $15.00 USD Received 9 Sep 2008; revised 10 Oct 2008; accepted 25 Nov 2008; published 15 Dec 2008

variation of r_1, the change of r_2 has a much larger influence on the even mode than on the odd mode: The band width is broadened by about 50% for the even mode but just 18% for the odd mode. The difference effects on the even and odd mode can be understood from the modal field profile of these two modes. As can be found in Fig. 3(a), the first side lobe of the modal field is located at the first row of air holes for the odd mode while it is concentrated on the second row of air holes for the even mode. A perturbation on the geometric configuration of a region where the local electromagnetic field energy concentrates can lead to a much more remarkable change to the mode feature than on the other regions. On the other hand, our numerical simulations show that the broadening of the transmission band width exhibits a saturation behavior upon the variation of r_1 and r_2. For r_1<50 nm or r_2>190 nm, the width of the transmission window barely increases when we further decrease r_1 or increase r_2. It seems that the modulation on the guided-mode band have their limitations by the current optimization scheme.

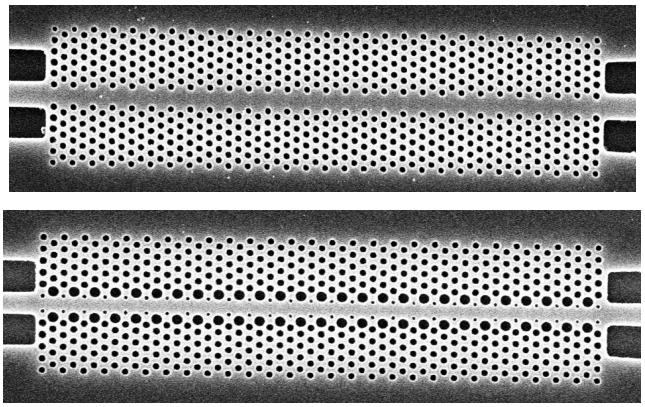

Fig. 4. SEM pictures of the fabricated Γ–M waveguide sample before (upper panel) and after (lower panel) optimization. The structural parameters for the two waveguides are a=430nm, r_1= r_2= r_0=120nm, w_d= w_0, and a=430nm, r_1=50nm, r_2=170nm, w_d =0.65 w_0.

In the above we keep the apparent width of the waveguide w_d unchanged. Now we further explore this additional structural freedom for optimizing the width of the transmission windows. We have investigated a series of waveguides with w_d varying from 0.65 to 0.75 w_0. The calculation results of guided-mode band diagram are displayed in Fig. 3(d). The effect of modulation is clearly seen in the dispersion curves. As w_d decreases while r_1=50nm and r_2=170nm, the width of the transmission window increase in the PBG region and finally reaches the maximum quantity of 50 nm at w_d =0.65 w_0. The frequency bandwidth is far broader than that in original Γ–M waveguide. Furthermore, it can be seen from Fig. 3(d) that at this parameter the even and odd band is almost free from overlap in frequency with the band width of the odd mode much broader than the even mode and as a result the single-mode operation is realized. This wide-band single mode feature is favorable for practical applications, e.g., in the wave division multiplexer.

#101332 - $15.00 USD Received 9 Sep 2008; revised 10 Oct 2008; accepted 25 Nov 2008; published 15 Dec 2008

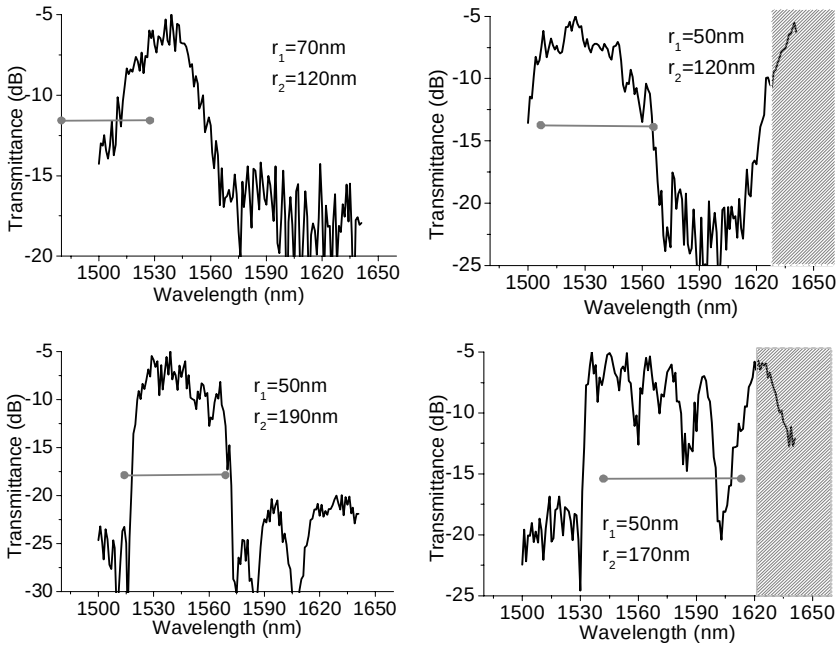

Fig. 5. Measured transmission spectra of several optimized Γ–M waveguides. The theoretical results of transmission windows of the entire guide modes are represented by the horizontal gray lines. Shadow areas represent the pass-band regions. In all the structures a=430nm and w_d=0.65w_0.

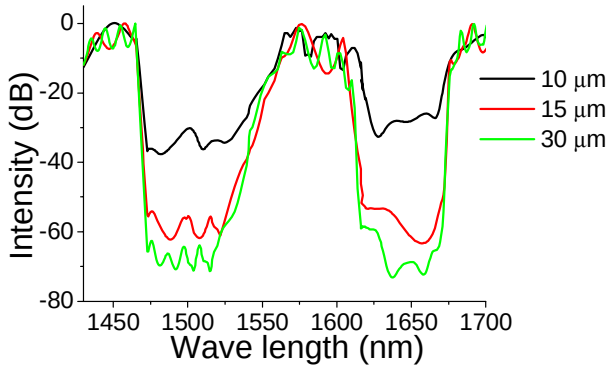

Fig. 6. Simulated transmission spectra of the optimized Γ–M waveguides with three different lengths. The structural parameters for the waveguide is a=430nm, r_1=50nm, r_2=170nm, w_d =0.65 w_0. The transmission intensities of the waveguide mode have the peak values of -0.1, -1.2, -1.3dB and minimum values of -12.9, -13.0 and -14.4 dB respectively.

Having had a clear picture of how to optimize the Γ–M waveguide through systematic numerical simulations, we proceed to realize the designed waveguide in experiment on the SOI slabs. The length of the modified Γ–M waveguides is 20μm (the same value as the original waveguide). The SEM picture of a typical optimized Γ–M waveguide sample is shown in the lower panel of Fig. 4. The subtle difference in structure from the original Γ–M waveguide sample [upper panel of Fig. 4] can be seen clearly. Figure 5 shows the measured transmission spectra of several optimized Γ–M waveguides. We measured the transmission

#101332 - $15.00 USD Received 9 Sep 2008; revised 10 Oct 2008; accepted 25 Nov 2008; published 15 Dec 2008

intensity of the same sample more than five times. The measured intensity fluctuation was less than 0.5dB. Distinctive transmission windows and cutoffs appear in the spectra. To facilitate direct theory-experiment comparison, we plot the theoretical result of transmission windows, including the "leaky" mode areas by gray lines. Compared with the calculated dispersion curve in Figs. 3(b), 3(c), and 3(d), the observed propagating band coincides well with our expectations, despite slight frequency deviations caused by the uncertainties in the fabrication process. Obviously, the width and position of the guided modes strongly depend on the parameters of r_1 and r_2. The "leaky" modes in Fig. 3 are verified again to be the low loss mode for their contributions in the observed transmission spectra. The optimized waveguides all have a high transmission band that is much broader than the original waveguide. Besides, the intensities of the transmission spectra are much higher than the original one. The maximal values almost increase more than 10 times: from –15dB to –5dB.

As the total loss for the optimized Γ–M waveguide is 5dB, the propagation loss for the 20μm long waveguide must be well below 5dB. To have a more quantitative value about the propagation loss level, we employed the 3D FDTD method to simulate the propagation loss of the pure Γ–M waveguide. Three waveguides with their length changed from 10μm to 15μm and to 30μm are tested, and the calculated transmission spectra are shown in Fig. 6. The boundaries of the gap and the mode region coincide with the dispersion relations in Fig. 2 and Fig. 3 and the measured transmission spectra in Fig. 5. The peak transmissivity values of the waveguide modes are -0.1, -1.2, -1.3dB and the minimum transmissivity values are -12.9, -13.0 and -14.4 dB, which also coincide approximately to the measurement data in Fig. 5. This result indicates that as the length of the pure Γ–M waveguide increases the intensities of the transmission barely change. The propagation loss for the leaky modes is estimated to be below 1.0 dB per 20μm. Overall, our results confirm that by fine tuning the geometric parameters of the structure we can realize wide single-mode transmission bands in the Γ–M waveguide in 2D triangular lattice PC slabs.

One may notice from Fig. 3 that in the optimized Γ–M waveguide the high transmission band still consists of a large fraction of leaky modes that lie above the light line and the lossless guided modes that lie below the light line still have a limited bandwidth. The reason is that the light line of the waveguide is very close to the Brillouin zone edge in the *k*-space due to the relatively large lattice constant ($\sqrt{3}a$) of the waveguide compared with the conventional Γ–K waveguide whose lattice constant is *a*. This leaves a very limited *k*-space for lossless guided modes to greatly expand the bandwidth. However, as has been shown both experimentally and theoretically in the above, the optimized waveguide has a relatively low loss in the whole wide transmission band, so such an optimized waveguide structure can still find applications in areas that do not require a very long propagation path of light signal.

4. Summary

In summary, we have investigated theoretically and experimentally the optical properties of Γ–M waveguides made in 2D triangular-lattice PC slabs. We have found that the original waveguide has a very narrow band width of guided modes. The band width can be significantly enlarged by modifying the radius of the air holes in the first and second rows adjacent to the waveguide core as well as the width of the waveguide core. Optical characterization of the fabricated waveguides shows good agreement with the theoretical prediction. As the Γ–M waveguide is perpendicular to the usual Γ–K waveguide, it offers an alternative to construct a waveguide interconnection beyond the usual scheme of Γ–K with Γ–K waveguides. A high-performance wide-band Γ–M waveguide should be of great help to build integrated-optical devices such as interconnection networks, channel-drop filters, and wave division multiplexers with more flexible geometrical configurations in 2D PC slabs.

#101332 - $15.00 USD Received 9 Sep 2008; revised 10 Oct 2008; accepted 25 Nov 2008; published 15 Dec 2008

Acknowledgments

The authors would like to acknowledge the financial support from the National Natural Science Foundation of China at Grant No. 10525419 and the National Key Basic Research Special Foundation of China at Grant Nos. 2006CB921702 and 2007CB613205

#101332 - $15.00 USD Received 9 Sep 2008; revised 10 Oct 2008; accepted 25 Nov 2008; published 15 Dec 2008